



Received: 10 July, 2024

Accepted: 18 July, 2024

Published: 19 July, 2024

*Corresponding author: Giulio Fanti, Department of Industrial Engineering, University of Padua, via Venezia 1, 35131 Padua, Italy, E-mail: giulio.fanti@unipd.it; giuliofanti@tiscali.it; fantigi@gmail.com

ORCID: <https://orcid.org/0000-0003-4584-4488>

Keywords: Human blood; Bloodstains; Erythrocytes; Creatinine; Fibrin; Urea; Pulmonary edema; Beta-activity; Fluorescence

Copyright License: © 2024 Fanti G. This is an open-access article distributed under the terms of the Creative Commons Attribution License, which permits unrestricted use, distribution, and reproduction in any medium, provided the original author and source are credited.

<https://www.clinsurggroup.us>

Check for updates

Review Article

New Insights on Blood Evidence from the Turin Shroud Consistent with Jesus Christ's Tortures

Giulio Fanti*

Department of Industrial Engineering, University of Padua, via Venezia 1, 35131 Padua, Italy

Abstract

After a critical revision of the main results obtained on the hematic material of the Holy Shroud in Turin, this paper presents various news of both a macroscopic and microscopic nature.

At a macroscopic level, news regarding the directions and position of blood and the probable presence of pulmonary fluid are discussed. Also, the bloodstains on the left arm are examined to try to distinguish different kinds of hematic fluid.

At a microscopic level, three different types of blood are evidenced. Hypotheses have been formulated to distinguish pre-mortem and post-mortem blood and to distinguish erythrocytes on the basis of their different sizes. The presence of fibrin, earthy material, creatinine typical of a tortured person, and the stacking of erythrocytes is also discussed along with their Beta-activity and fluorescence.

Finally, the physical conditions relating to Jesus are discussed from a medical point of view which could explain all the news of the hematic material taken from the HST and are consistent with the tortures of Jesus Christ described in the Holy Bible.

1. Introduction

A few studies [1-9], show that the Holy Shroud in Turin (HST) is a handmade 3:1 twill linen cloth, 4.4 m long and 1.1 m wide, on which the front and back images of a human body are permanently and mysteriously imprinted [4,5,10,11]. According to Pope Julius II (who approved the Mass and the Office of the HST in 1506) and the subsequent Catholic Christian tradition, the HST is the burial cloth in which the body of Jesus Christ was wrapped before being placed in a tomb in Palestine about 2000 years ago, see Figures 1,2.

The Catholic Christian Church does not impose any veneration requirements of the HST, even though science has been unable to refute what is reported by tradition.

There are some indications that the HST was in Palestine in the first century A.D., and then taken to Edessa (present-day Sanliurfa in Turkey) but other scholars hypothesize different paths for this Relic [9,12].

Several features found on the facial image on the HST accurately coincide with those found on depictions of Christ on Byzantine coins starting from the VII century A.D. which provides evidence that the HST was seen during the Byzantine Empire [9]. After disappearing during the Sack of Constantinople in 1204, the "Shroud of Christ" then, later, appeared in Europe in 1353 in Lirey in France. In 1532, a fire damaged it at Chambéry in France. In 1578, it was taken to Turin where it has remained until now, apart from some short periods of time when it was hidden during wartime.

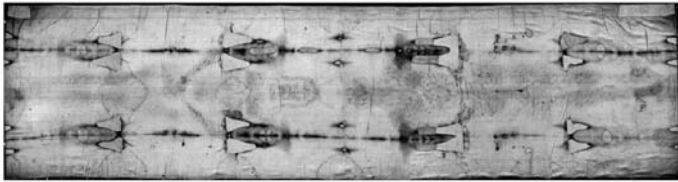


Figure 1: HST photographed by G. Enrie in 1931.



Figure 2: Manikin obtained from a deep study of the HST where the author painted in white the human body parts not imprinted on the HST due to incomplete wrapping.

The HST shows a particularly unusual double human body image which still cannot be explained due to its unique combination of features [1,4,5,10,13,14] which have, so far, proven to be impossible to reproduce.

Nevertheless, many hypotheses have been formulated [10] that propose how this image may have been formed. According to the Author and other experts, the most plausible explanation is that it was produced by an energy of unknown origin, also of an electric type [1,13] probably connected with the Holy Fire of Jerusalem which emanated from the corpse and reacted with the linen of the HST. The irregular distribution of radiation along the surface of the HST would have produced both the body image and an isotopic alteration of the atoms in the fabric which varied along its surface.

Numerous bloodstains [1-5] scattered throughout the double body image of the HST show evidence that Jesus of the HST was tortured [15]: bloodstained marks all over the body image which are consistent with pre-crucifixion flagellation, bloodstained marks on the head that are consistent with a "crown" of thorns, blood marks on the hand and feet that are consistent with crucifixion and the bloodstain on the chest that evidences a post-mortem wound that corresponds with the post-mortem spear wound that Christ received as is described in the Bible.

In 1988, the HST was radiocarbon-dated to 1260–1390 A.D. [16], but the result is questionable [2,17–24] also in the light of the new results discussed in Sections 6.1 and 7.

A piece of linen (officially 7 cm long and 1 cm wide) was cut from the Relic and given to laboratories in Oxford, Zurich, and Tucson (Arizona) laboratories for radiocarbon dating. Each laboratory measured the $^{14}\text{C}/^{12}\text{C}$ isotopic ratio to assign an

age to the samples. Whether there was true independence in the radiocarbon dating between these three laboratories, the statistical procedure followed and the underestimation of the systematic effects is highly debated.

As the process that formed the body image is still unknown, the dating method cannot be rigorously applied, because the environment in which the object under analysis was conserved must be known from a contamination point of view. The imaging mechanism may have varied the percentage of carbon isotopes of the HST which might have produced a non-negligible systematic effect.

This paper focuses attention on the numerous bloodstains present on the Relic, especially in correspondence with the body image which correspond in shape and position to the numerous tortures suffered by the Man, recognized as Jesus by the author, who was wrapped in it.

The composition of these red spots has been discussed for several decades, but it has not yet been fully clarified. However, there is now no doubt that they are composed of hematic material.

Therefore, in this work, after a commented synthesis of the studies carried out in the past, some interesting news is presented both from a macroscopic point of view and a microscopic one.

2. Commented history of blood detection

On the HST, there are hundreds of reddish spots of varying shapes and sizes from centimeters to a few decimeters which almost completely overlap the body image imprinted on it and which seem perfectly consistent with the different types of torture suffered by Jesus who was wrapped in it as a corpse.

The problem of the experimental identification of the different reddish spots present on the HST was initially addressed by the Diocesan Commission of Card. Pellegrino (magazine: *La Santa Sindone, Ricerche e studi ... della Commissione Pellegrino del 1969, Suppl. Riv. Diocesana Torinese* 20 January 1976). In 1973, this Commission sampled and studied some specimens removed from the cloth, and these experts were the first in the world to identify blood particles in the samples taken from HST linen threads that were impregnated with the reddish substance in question, although they did not recognize what they were looking at (Guido Filogamo and Alberto Zina on Page 56). In fact, the final result of the Commission was inconclusive about whether or not blood was present in the samples or not.

After an examination with SEM (Scanning Electron Microscope), but not connected at those times with an XRF detector (X-Ray Fluorescence), Filogamo and Zina wrote the following which would have allowed the knowledge of the element composition: "On the surface of the fibers or close to it, various formations of various structures, shapes and sizes can be observed. We detected three different types:

1. Granules of electron-dense amorphous material

II. Rounded or oval bodies of 0.5-0.7 microns in which an external capsule, a membrane and an opaque central portion are evident

III. Rounded bodies of 2 microns in diameter apparently surrounded by a membrane and made up of fine granular material unevenly distributed and of different electronic density.

Type I material is of an unspecified nature. Due to their characteristics, type II bodies can be identified with certainty as bacterial spores.

Given their internal structure, type III bodies are likely of an organic nature. ... The possibility that these formations are red blood cells cannot be excluded ... but some characteristics: dimensions, appearance of the granulations, make us consider this possibility unlikely."

As afterwards reported, Type I, electron-dense amorphous material correspond to the rarer particles of iron oxide (red ochre), mercury sulfide (cinnabar), and earthy dust due to contamination [3,25]. Type II and III, instead, very probably correspond to erythrocytes from different types of pre-mortem and post-mortem blood, and they, in fact, appear red if viewed with an optical microscope. The aforementioned material is composed of elements (carbon, oxygen, potassium, chlorine, sodium, sulfur, iron, and others) that are compatible with blood.

Since this study proved inconclusive, other investigators took additional samples from the HST and studied them with different methods.

Heller and A. Adler of STuRP (Shroud of Turin Research Project), [26,27] as well as others, [28] detected the presence of blood in 1980 by testing reddish particles that had been sampled from the sticky tapes put in contact with the HST. However, Heller and Adler focused their analysis on the chemical compounds forming the reddish material under analysis.

They obtained positive results for blood from the following methods: detecting the Soret Band at 410 nm (indicative of porphyrin in heme), EDX (Energy Dispersive X-ray Analysis), protease test, protein test, identifying organic matrices, detecting bile pigments, hemochromogen test, micro-spectrophotometric test, fluorescamine test for amines and peptides, identifying albumin in the areas where serum halos appeared, and the hydrazine to distinguish blood particles from iron-oxide particles.

P.L. Baima Bollone in 1982 [29] independently detected the presence of human blood on the HST. Studying the blood material impregnated in the filaments coming from the HST, he also found the presence of a corpuscle which, from its shape, he identified as an erythrocyte (Sindon n. 33, 1984: Further research...). However, this rounded particle was 14 micrometers in size which is very different from human erythrocytes which are about 7 micrometers in size.

Gerard Lucotte [30] confirmed Baima Bollone's finding having detected the presence of erythrocytes up to 13 micrometers in size, but he also found smaller erythrocytes up to 6.5 micrometers in the analyzed HST samples.

The fact that G. Lucotte himself published these results in a scientific paper which was subsequently retracted and given that the erythrocyte found by P.L. Baima Bollone had not found confirmation of repeatability suggests that this material could also be due to external contamination.

In sharp contrast, analyzing the same samples collected by STuRP and studied by Heller and Adler, W. McCrone [31-37] detected no blood whatsoever on the HST, but, instead, he identified very small-sized red pigments (like red ochre and vermilion) which he referred to as "Sub-Micron Particles (SMP.)" McCrone claimed that these SMP were the source of the red images of the HST.

This finding is in agreement with the Type I particles identified by Zina and Filogamo in 1976 ("granules of electron-dense amorphous material"), because the claimed red ochre and vermilion particles identified by McCrone are easily determinable in the SEM-EDX analysis, precisely because they show a higher density than other, more frequent, blood particles.

However, it is strange that a famous microscopist like McCrone did not also consider the Type I and II particles already identified in 1973-76 which, according to the author, are also very preponderant [3,25] compared to those that McCrone has repeatedly declared (in a way much discussed even by experts of the sector) [26-28], as being the only source of the reddish coloration of HST spots. In fact, a study [3] shows, based on both X-ray photos described [7] and on experiments born from the results detected [8], the insufficiency of red pigments like red ochre and vermilion to produce a visible image on the HST.

This study [3] adds other information about the blood on the HST, among them the following:

- As the bloodstains on the X-ray photo [7] are absent, it results that (a) both the body image and the bloodstains visible on the HST are not produced by pigments; (b) the detected presence of SMP of iron oxide and mercuric sulfide, probably due to transfer from the painted copies of the HST being pressed against the Relic, can be excluded as the source of the red matter on the HTS.
- The volume percentage of blood on a single colored fiber is greater than 90% while that of SMP is less than 10%, thus showing its absence of influence in the bloodstain coloration.
- The source of the red color of bloodstains is due to the porphyrins (and not iron) which give hemoglobin in blood its characteristic red color.
- The bloodstains on the HST have remained curiously reddish in color for many centuries, and the relatively low areal density of SMPs is insufficient to explain the

reddish color of the HST blood. Several hypotheses have been formulated to explain the still-red bloodstains on the HTS, but none of them seems fully convincing. This paper will present a more reliable one. P.L. Baima Bollone, et al. [38] hypothesized that the red color of the bloodstains on the HST is due to carbon oxide produced by the breakdown of erythrocytes (due to the torture) which would have bound to hemoglobin to produce carboxyhemoglobin so as to sustain the blood's reddish color. C. Goldoni [39] and A. Di Lascio, et al. [46] supposed a high bilirubin content (due to torture) which, with the additional exposure of that blood to a sufficient dose of UV rays, has sustained the reddish color.

Finally, a study [2] illustrates the reported Phillips' hypothesis reported [19,20] which assumed that neutron radiation on the HST would have transformed the nitrogen and ^{13}C nuclei into ^{14}C , thus heavily skewing the results of the radiocarbon dating of the HST performed in 1988 [16] by many centuries.

This study [2] therefore found confirmation of the hypothesis of neutron irradiation which altered the isotopic percentage of the carbon atoms of the linen present in the Relic, reporting that, unlike common human blood which contains nitrogen (percentages by weight of the order of 10%), the blood nitrogen level of the HST is lower than the background noise of the instrument (about 1%).

Obviously, this neutron flux might have also influenced the color of blood.

3. Materials and methods

As regards the analyses carried out from a macroscopic point of view, the high-resolution digitized photographs of G. Enrie (1931), G.B. Judica Cordiglia (1969), and G. Durante (2000, 2022) were studied. These were studied using Jasc Paint Shop Pro 7 and ImageJ 1.53k image processing software.

As regards the analyses performed from a microscopic point of view, a list of sample instrumentation follows.

STuRP tape samples and dust vacuumed from G. Riggi di Numana (with an unbroken chain of custody since 1978) were used by the author to pick up the following specimens recognized by him from optical and element analysis.

- GF-3EF-1 and GF-3EF-2: pieces of sticky tape taken from sample STuRP-3EB (wrist area, frontal image of the HST) about 1 mm in size containing micrometric particles of Type A blood; the mass of the blood crusts was respectively evaluated as 50 (+50 -30) ng and 70 (+50 -30) ng.
- GF-3EF-3: a triangular piece of sticky tape taken from sample STuRP-3EB containing various particles and fibers.
- GF-1HB-1 and GF-1HB-2: a piece of sticky tape taken from sample STuRP-1HB (feet area, dorsal image of

the HST) about 1 mm in size containing micrometric particles of Type A blood; the mass of the blood crusts was respectively evaluated as 60 (+60 -30) ng and 100 (+100 -60) ng.

- Filter-f, Filter-h, and Filter-i of dust vacuumed from the back-side image of the HST by G. Riggi di Numana in 1978, respectively in correspondence of face, gluteal area, and left upper corner of radiocarbon area.
- "h-S": linen fiber coming from Filter-h.
- GF-h18-3a and GF-h18-3b: two sherds of Type B blood coming from Filter-h, total mass respectively of 1.5 ± 1.0 mg and 3.0 ± 1.0 mg. During tests, sample GF-h18-3a was fractured in two parts.
- For analyses using electron microscopes, some individual micro-samples coming from 3EF and 1HB sticky tapes were previously mounted on appropriate stubs and metallized with gold or chrome.

Detailed description of Type A, B, and C blood will be done in Section 5. It must be noted that the material listed (but not mentioned in the following Sections) was used for the reproducibility analysis of the results obtained.

Tape 3EF was put in contact with the wrist area of the frontal image of the HST by R. Rogers of STuRP in 1978, while Tape 1HB was put in contact by him with the feet area of the dorsal image of the HST.

The samples were first recognized and isolated from the rest of the material by the author using an Olympus zoom stereomicroscope, and then they were analyzed with a polarizing optical microscope in reflected and transmitted, visible and UV light with magnifications up to 1500x.

Further analyses were performed with the employment of SEM (Scanning Electron Microscope), ESEM (Environmental Scanning Electron Microscope), and SEM-FEG (Field Emission Gun). Raman analysis was performed to evidence the hemoglobin which is typical of blood.

The element weight percentages of the particles in question were determined via XRF-EDS (Energy Dispersive X-ray Fluorescence Analysis) which is also called EDX (Energy dispersive X-ray spectroscopy), and, finally, a preliminary analysis of the ionizing radiations Alpha, Beta, and Gamma [40] were also performed.

All this sophisticated equipment has been employed to study more in-depth the samples in question whose red coating had, since 1976, posed various interpretative difficulties for the Diocesan Commission due to its complexity.

Various reddish SMPs of red ochre and vermilion are mixed with the blood material due to the probable contamination of the HST with copies placed in contact after their production [3,25]. To these, we must add various sub-micrometric particles typical of a calcareous-clayey soil similar to that of Jerusalem. Such dust could easily get onto a body that has fallen to (or

been pushed onto) the ground such as when someone is beaten and then crucified.

These particles are not the subject of the present analysis which, instead, focuses on three different types of blood substances which, via the Gospels, can be correlated to different moments of the Passion and Death of Jesus.

4. Macroscopic news on blood

It is not easy to correctly interpret in detail all of the bloodstains present on the HST, and this is why their study is constantly evolving. Here, below, is new information derived from recent studies carried out by the author with the help of various collaborators.

4.1 Probable fluid due to pulmonary edema leaking from the side wound

A preliminary study not yet published, carried out with engineer Christian Privitera, has highlighted the presence of an almost transparent substance in the interstices between the threads of the cloth in the bloodstained area bloodstains of the side wound.

This substance, given its origin and in agreement with other scholars who have analyzed the Shroud of Oviedo, could be the semi-transparent fluid produced by pulmonary edema.

In fact, Figure 3 shows a colorimetric analysis, using the CIE XYZ color space (Tristimulus values defined by the International Commission on Illumination that includes all color sensations visible to a person), of some points of the photo of the side wound.

Points H-I-L-M-N-O correspond to bloodstained areas that are far in the plot from Points P-Q-R-S-T of the background showing the clear difference in the color of the photo. The Points B-C-D-E-F-G of the interstices among the bloodstains are also separated in the plot from the background color, thus, sustaining the hypothesis of the supposed semi-transparent fluid produced by a pulmonary edema.

4.2 Direction of the bloodstains on the side

The HST (photo by G. Durante in 2000) shows, in correspondence with the bloodstains of the side on the frontal image, different directions of the flowing blood that can be grouped into three: a vertical one with the human body in the upright position, a second one inclined of at about 45° from the vertical, and a third one considering the corpse lying down and resting on its side, see Figure 4 [41]. As the single rivulets show a sudden change of their direction, it is probable that the blood flows streamed when the corpse was moved.

These flows of blood could have varied their direction during the deposition, the transportation of the corpse to the sepulcher, during the quick funeral preparation in the sepulcher, and from possibly rotating the body so as to cleanse it before burial.

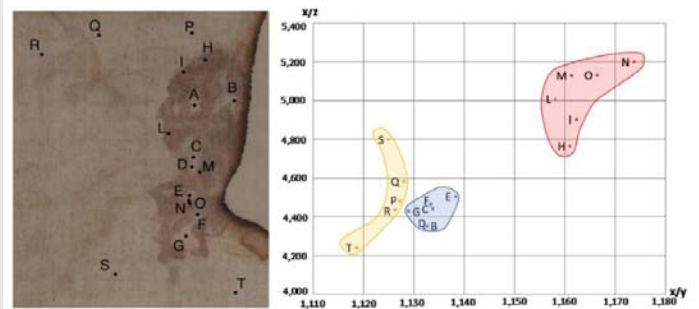


Figure 3: On the right, plot in the CIE XYZ color space of the points reported in the photo of the side wound shown on the left.

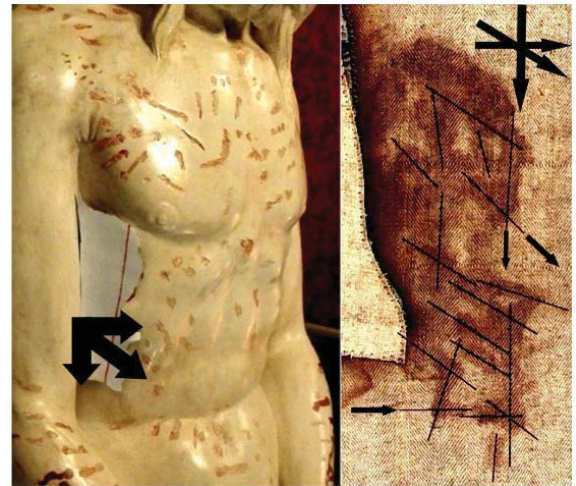


Figure 4: Three principal directions of the blood pattern were detected in correspondence with the side wound on the right (photo mirrored). The white paper model represents the side wound posed on a life-size sculpture.

4.3 Different kinds of hematic fluids on the left arm

Bloodstains on the HST have different macroscopic characteristics; we consider for example those of the arms which are caused by the rather apparent nail wound in the left hand wrist area.

Figure 5 on the left highlights three different types which are characterized by different colors. The most evident traces (indicated by the blue spot in the figure) appear to be postmortem blood leakage which probably occurred due to the movement of the corpse during transport or in the tomb and which transposed into the HST in a liquid phase; the less evident ones (indicated by the red spot in the figure) seem to be pre-mortem bloodstains which probably occurred when Jesus was still nailed to the cross and which were transposed onto the HST after the blood crusts dissolved due to fibrinolysis [42] in the humid environment of the sepulcher; the traces evident under ultraviolet light (indicated by the yellow spot in the figure) appear to be leaks of blood serum (as we see also on the right foot of the dorsal image of the HST) which occurred due to the capillary action of the serous component of the post-mortem blood, more active than the red corpuscular part of the blood.

Figure 5 on the bottom right shows the bloodstains in greater detail and highlights the probable square-section hole

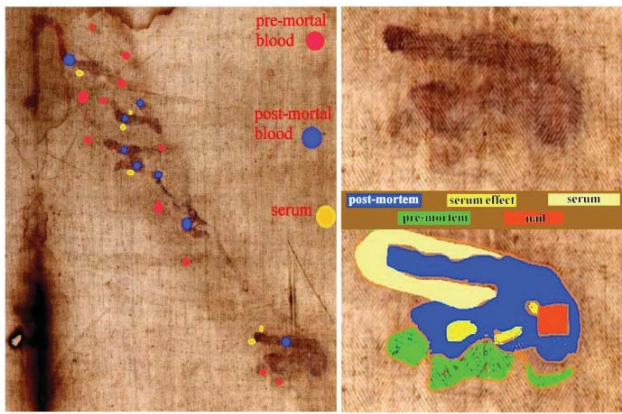


Figure 5: On the left, is a proposed classification of bloodstain types on the left arm of the body image; on the right, is a detailed characterization of different bloodstains on the hand-wrist area.

of the nail and the probable concentration of serous liquid between the post-mortem blood drips.

4.4 Bloodstains out of body image and scourge marks on the head image

The bloodstains produced by flagellation that are visible on the HST hide a lot of information that, little by little, comes to light if the study is deepened.

For example, the author, in developing an observation of lawyer Theodora Pappas - who is writing a book about the blood on the HST - considered Figures 6-1 and 6-2 which highlight a fact apparently difficult to explain: in correspondence with the right shoulder of the dorsal image, there is at least one scourge wound that is external to the body image.

It is obvious to think that the blood was transferred onto the HST by skin-sheet contact. Therefore, at first sight, it does not seem easy to explain why the bloodstains exist in some areas like this of the right shoulder (or also in correspondence with the knees of the dorsal image) but are not superimposed to the body image. In fact, we know that the latter was formed by radiation even in areas not in contact with the body sheet, but the bloodstains require a body sheet contact.

The answer, which also confirms the still incomplete hypothesis regarding the formation of the body image [1,13], refers to the fact that if we consider a floating body immersed in a vertical electric field, the intensity of this field is proportional to the cosine of the angle defined by the perpendicular direction of the body surface and the vertical direction.

It is therefore obvious that in correspondence with the rounded shape of the shoulders, this angle tends to 90° , thus bringing the local intensity of the radiation that caused the body image to zero, but the skin-sheet contact still allowed to form the bloodstain in question.

The scourge wounds are more abundant on the back, but the whole human body is dotted with such wounds; the author counted 372. However, it should be noted that a single bloodstain that appears as a scourge mark (as opposed to a

blood flow from a “crown of thorns”) is, also, evident on the head, see Figure 6-3 of the dorsal image, and this is confirmed by the similarity with other scourge marks shown in Figure 6-4.

This suggests that even the right eye, more sunken and with the eyelid apparently furrowed by a vertical mark, could have been blinded by another blow of the scourge on the head. As an alternative to the scourge mark on the right eye, one can think of a wound produced by a thorn from the crown placed on Jesus' head.

4.5 Blood quantity necessary to stain the HST

In observing the HST, many have commented that a lot of blood must have been shed in order to account for the number of bloodstains that are on the HST and that a corpse could not have shed such a quantity of blood.

However, a simple experiment reported in Figure 7 highlights the opposite: only 3 cm^3 of colored fluid was poured onto a linen fabric similar to the HST. The life-size photo in the figure compares the area of linen fabric soaked in this quantity of colored liquid with that of the side wound of the HST.

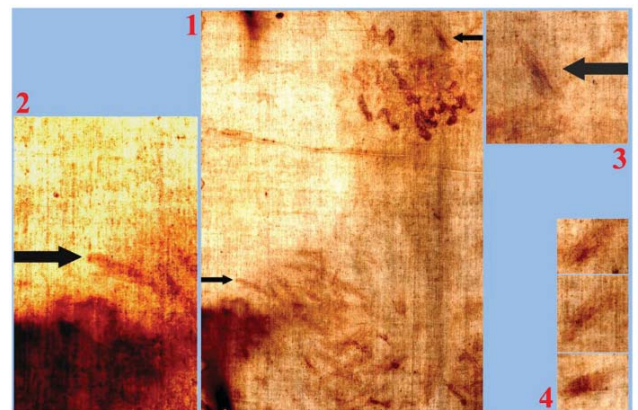


Figure 6: 1. Dorsal image of the HST comprehending right shoulder and head. 2. Detail of bloodstain out-of-image on the right shoulder. 3. Detail of scourge wound on the head. 4. Other scourge marks on the HST for comparison.



Figure 7: Life-size photo comparing the side wound (on the right) with the area of only 3 cm^3 of colored fluid soaking a linen fabric similar to the HST.

Some might argue that the fluidity of the colored liquid used for the experiment was much greater than that of the blood-soaked in the HST, but this experiment only served to qualitatively show the quantities of fluid that could have affected the two fabrics.

From a very approximate evaluation, it can therefore be stated that a quantity of blood less than 10 cm³ was most likely sufficient to stain the entire Relic.

5. Microscopic news on blood

After some news on bloodstains analyzed from a macroscopic point of view, we now enter into the microscopic detail that seems less studied principally due to the relative scarcity of blood material available to scholars who are consequently oriented towards other types of studies. Blood particles will be subdivided here into three categories: Type A, B, and C, based on their microscopical appearance.

5.1 Type A blood: Microparticles

Type A blood is typical of that sampled by the sticky tapes placed in contact with the HST by R. Rogers during the 1978 STuRP campaign, and it is very similar to what was published by Kohlbeck, et al. [43]. It consists of numerous reddish particles present in the sticky tapes both adhering to the HST linen fibers and isolated in the tape's adhesive. The elemental composition of this material is compatible with that of blood particles.

The color of these particles is orange-red when observed under an optical microscope, and the green color of some particles is due to optical problems of refraction and dispersion of incidental light in the microscope. Most of these particles adhere to the fibers sampled in the tape, see Figure 8a and 8b, but some are dispersed directly into the adhesive or grouped into agglomerates, see Figure 9.

The appearance of these rounded discoidal particles is like a donut with central concavity, and it is very similar to that of an erythrocyte, see Figure 10 where elements contained therein are compatible with those of blood: among other elements, Carbon-C, Oxygen-O, Iron-Fe, Calcium-Ca, Chlorine-Cl, Nitrogen-N, Potassium-K, and Phosphorus-P were detected. Silicon-Si is due to the supporting glass, and Gold-Au is evident because the sample was previously metallized with Gold. Figure 11 shows a sectioned particle having a diameter of 500 nm which is very similar in shape to an erythrocyte.

These particles of Type A blood make one think of erythrocytes, or parts of them, found in human blood (however having sizes of 7 micrometers). As their sizes range from 0.3 to 2 micrometers with a prevalence of 0.7 micrometers, we, therefore, can suppose that the particles under analysis can really be shrunken erythrocytes or parts of them.

Observations under the optical microscope using the Becke line confirmed that the rounded particles in question are composed of material compatible with blood and not with iron oxide as hypothesized by some scholars [31-37]. In fact, their

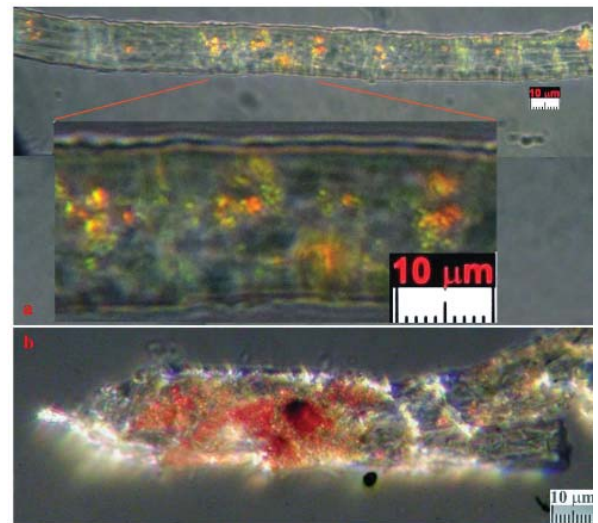


Figure 8: a. Countless particles, mostly sub-micrometric, with rounded donut shapes from sticky tape GF-1HB-1 (feet area of the dorsal image), epi-illumination in the gray field. b. Countless particles also grouped in agglomerates from sticky tape GF-3EF-3 (wrist area, frontal image), epi-illumination in the gray field.

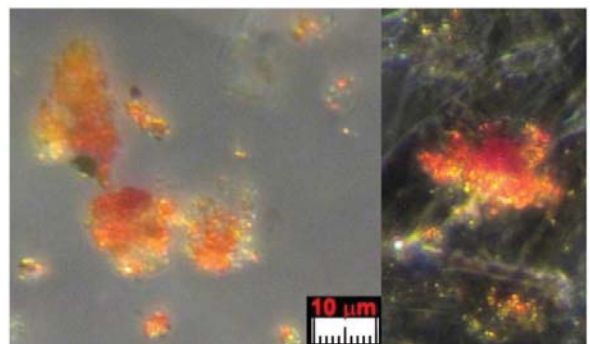


Figure 9: Sub-micrometric particles dispersed in the adhesive, or grouped in agglomerates, with a rounded donut shape from sticky tape GF-3EF-1 (wrist area, frontal image) on the left and GF-1HB-1 (feet area of the dorsal image) on the right, epi-illumination in the gray field.

refractive index was lower than that of balsam oil having 1.515 and, therefore, incompatible with that of iron oxide (which has a refractive index of 2.5 - 3.2), but which is compatible with the refractive index for blood (which is 1.34 - 1.37).

Two hypotheses can be formulated from the analysis of particles shown in Figures 8-11 named microcytes. Either they derived from uncoagulated blood that underwent strong shrinkage (preferred by the author) or, alternatively, these particles could be apoptotic bodies that resulted from echinocytes (erythrocytes that have short and rounded protuberances indicating a pathology such as uremia) that have fragmented and scattered in the plasma.

Prof. Rosa Boano of Turin University and Prof. Ezio Fulcheri suggested to the author to consider the possible shrinkage of erythrocytes due to drying in a millennia-old-fabric like the HST, and they furnished to the author a paper by Rabino-Massa, et al. [44] who in 1967 studied the possible shrinkage of erythrocytes due to drying in Egyptian mummies and found erythrocytes in the blood of a softened and rehydrated scalp of a mummy. They found rounded discoidal elements with central

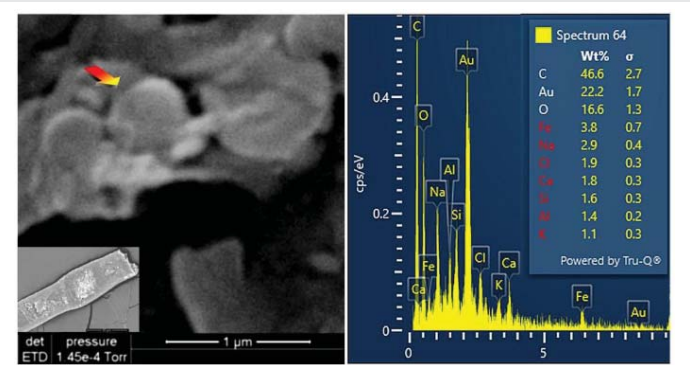


Figure 10: Sub-micrometric blood particles from sticky tape 3EF (wrist area, frontal image) with elemental analysis showing components compatible with blood.

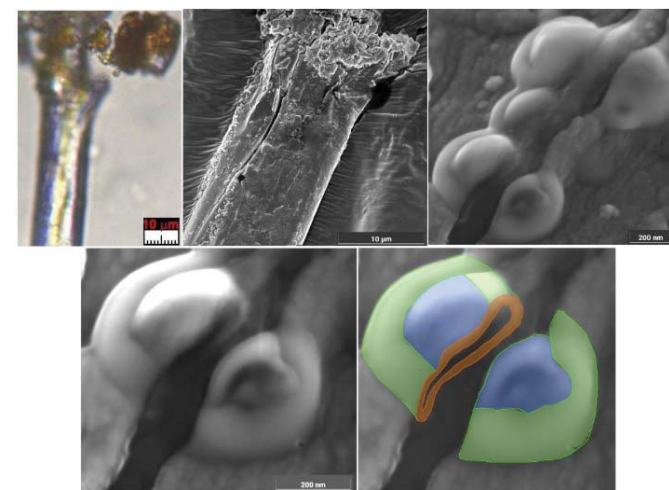


Figure 11: Sectioned sub-micrometric blood particles "h-S" from Filter-h showing a geometry very similar to that of an erythrocyte but having a diameter of about 500 nm. As seen on the top linen fiber with an optical microscope (on the left) and SEM (on the center), there is evidence of a crack (on the right); on the bottom, detail of particle of Type A blood (on the left) colored (on the right) to evidence the sectioned structure typical of an erythrocyte.

concavity and with a diameter of 4–5 micrometers. Therefore, one can think that the same non-hydrated erythrocytes could have dimensions smaller than those measured.

Experimental tests performed by the author with human blood mixed with urea, aloe, and myrrh showed that erythrocytes can shrink much more than what was found in Egyptian mummies.

Figure 12 shows the selected results of many experiments performed by the author in different conditions. In particular, he found a saturated solution of urea causes erythrocytes to be reduced to particles even smaller than a micrometer.

Incidentally, given that Jesus was suffering from very high uremia due to the flagellation which probably induced kidney (and also liver) failure, this transformation of the erythrocytes causing microcytic anemia, suggests the extreme difficulties He had in exchanging oxygen which most likely resulted in extremely labored breathing. As reported in Section 5.5, the high levels of creatinine detected in blood Type A, which is also coupled with deterioration of platelet function can be easily explained by this supposed kidney failure.

Finally, noteworthy is the fact that no whole leucocytes were found in this Type A blood, which is typical of a living person.

Particles of Type A blood, therefore, suggest their identification with post-mortem blood that came into contact with fluids probably rich in oils, aloe, and myrrh as well as urea exuded by the corpse which prevented coagulation. It appears as uncoagulated blood subjected to a strong shrinkage.

5.2 Type B: sherds of blood crusts

Type B blood has been prevalently found in Filter-f (Figure 13) and Filter-h (Figure 14) and consists of compact, but brittle, sherds of crusts of a darker color than Type A blood. It is rarer than Type A blood and therefore less easy to characterize.

Its element composition is compatible with that of blood, its size is up to a tenth of a millimeter and it has shapes that are not rounded but with edges that suggest previous fragmentations of larger particles. Other smaller sherds, with sizes of the order of a few micrometers, have been also observed in GF-3EB-3 and GF-1HB-1 sticky tapes.

This Type B blood does not appear to contain the typical microstructures of the red blood cells found in Type A blood. This fact leads one to think that it is pre-mortem blood that coagulated on the skin from open wounds when Jesus was still alive and that it was not mixed with the anti-putrid aromatics used for the burial of the corpse.

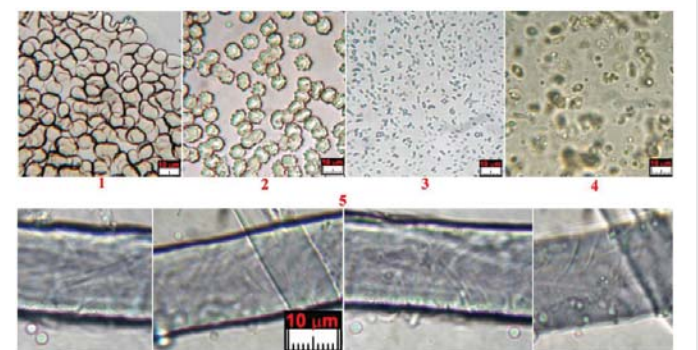


Figure 12: Selected tests performed with human blood showing erythrocytes. 1, blood smear on glass; 2, echinocytes deriving from erythrocytes smeared on glass; 3, human blood in saturated urea solution; 4, human blood mixed with a solution of aloe and myrrh; 5, enlargement of flax fiber immersed in a physiological solution and urea.

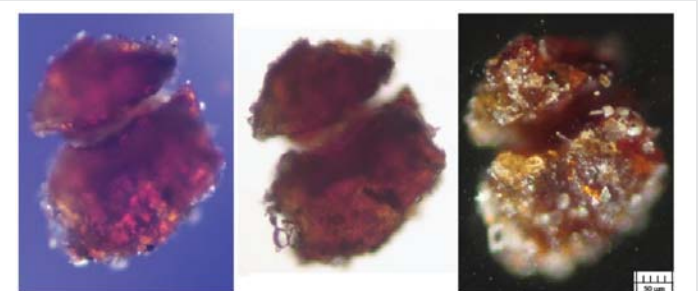


Figure 13: Sherds GF-h183a (smaller on the top) and b (bigger on the bottom) of Type B blood coming from dust vacuumed from the HST in correspondence with the gluteal area, seen in cross-polarized light on the left, in transmitted light on the center, and in epillumination on the right.

Raman analysis performed on the sherd of Figure 13 shows a partial burning on one side (presence of carbon composites) leaving us to think that this sherd could come from an area very close to the damage caused by the fire of Chambéry in 1532. Given its origin in the gluteal area, it is, therefore, easy to think that this sherd came from the “blood belt” of the back where burn holes in the linen fabric on both sides of the “blood belt” are visible. In fact, charred linen fibers from that area translocated to the gluteal area due to the folding and unfolding, and the rolling and unrolling, of the HST and have been detected in the dusts of Filter-h.

5.3 Type C blood: erythrocytes having sizes from 2 to 5 micrometers

Type C material consists of very rare donut-shaped particles found only from the dust of the HST vacuumed from the back side of the face (Filter-f).

The composition of these particles has not yet been determined because of a shortage of material to test, as well as because they are embedded in the sticky tape’s adhesive, and we did not want to risk damaging the particles.

The particle sizes range from 2 to 5 micrometers, and they have rounded donut shapes which is a structure that is compatible with that of erythrocytes, see Figure 15. These particles are currently too few to be definitively distinguished from possible bacteria, but they appear to be erythrocytes which did not coagulate due to an oily substance which may have been copiously applied to the face of Jesus whose body was wrapped in the cloth.

Figure 16 shows the SEM photo of a supposed echinocyte. Their larger dimensions compared to those of the Type A material could be explained by the fact that these particles were scattered on the skin when Jesus was not yet in the final phase of the supposed uremia, and, therefore, the erythrocytes never completely shrank in size.

5.4 Presence of fibrin

It is appropriate to add some other news. In some bloody fibers of HST, such as those resulting from wrist wounds (sticky tape 3EF), together with erythrocytes, traces of supposed fibrin are also evident, see Figure 17.

5.5 Presence of creatinine

The presence of nanoparticles ranging from 50 to 200 nm recognized as creatinine (already mentioned with ferritin in a paper retracted for reasons the author disagrees with [45] was detected in various bloody fibers of Type A such as those of the wrist area (sticky tape 3EF) and of the gluteal area of the dorsal image, see Figure 18.

As reported in the cited paper, the presence of numerous creatinine particles with ferritin confirms at a microscopic level the very heavy torture suffered by Jesus of the HST.

5.6 Stacking of erythrocytes

In some cases, such as that of Figure 19, particles

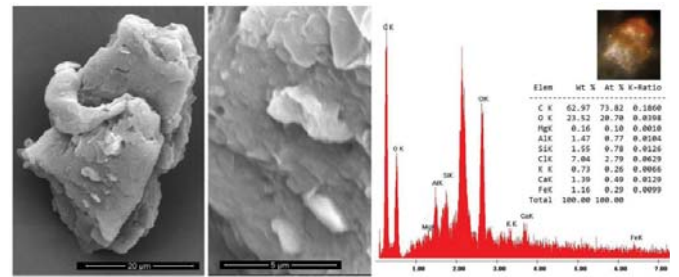


Figure 14: Sherd of Type B blood coming from dusts vacuumed from the HST in correspondence with the face area, Filter-f, with EDX elemental analysis on the right.

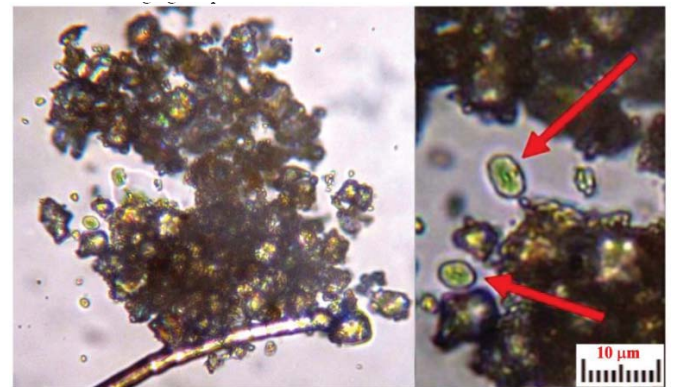


Figure 15: Particles of Type C blood of various sizes from 2 to 5 micrometers coming from dusts vacuumed from the HST in correspondence of face, Filter-f (glass #4-13).

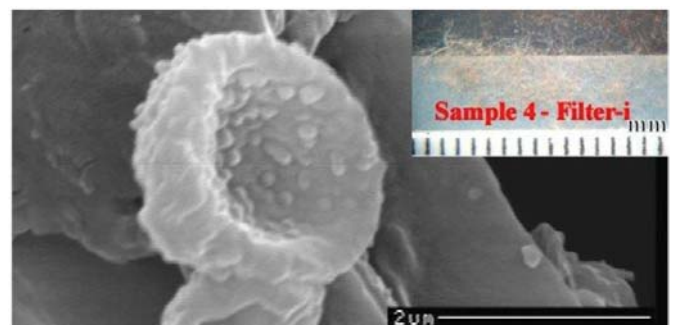


Figure 16: Supposed erythrocyte of Type C blood, about 3 micrometers in size, coming from dusts vacuumed from the HST in correspondence to the left upper corner of the HST Filter-i.

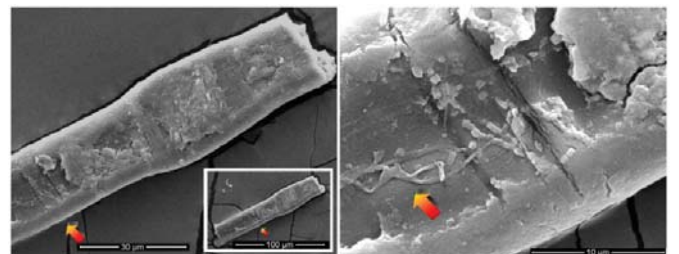


Figure 17: Fibrin filaments on the surface of a bloody fiber, sticky tape 3EF.

recognized via elemental analysis as blood particles (also due to their composition containing about 0.6% iron by weight) are observed as not scattered on the surface of the linen fiber, but *stacked together*.

This fact is in agreement with their Beta-activity as is discussed in Section 7 which demonstrates that electrically charged erythrocytes tend to arrange themselves along the lines of the electric field hypothesized in the Sepulcher of Jerusalem.

5.7 Presence of earthy material

Particles of earthy material typical of that found in Jerusalem, such as clay and limestone, (supporting the hypothesis that earthy dust remained on the body of Jesus because He was not completely washed) are frequently mixed with blood particles and with other particles of red ochre and vermilion, probably due to contamination from contact with painted copies of the HST (to transform them into relics in this way), see Figure 20.

6. Ionizing radiations of blood

When ionizing radiation passes through matter, it carries enough energy to release electrons from the affected atoms or molecules, so as to ionize them. They can be composed of subatomic particles, ions, or atoms moving at high speeds, or even electromagnetic waves. These forms of radiation are of the following different types: Alpha, Beta, Gamma, X-rays, and neutrons.

Alpha particles are made up of two protons and two neutrons bound in a particle identical to a helium nucleus without its two electrons. Alpha particles make up about 11% of cosmic rays and they are blocked by a paper sheet.

Beta particles are electrons, or more rarely positrons, of great kinetic energy, which are emitted by some radioactive nuclei, such as Potassium-40. These particles are significantly reduced by an aluminum foil.

Photon radiation is called Gamma rays if produced by a nuclear reaction, however, photon radiation is called X-rays if produced outside the atom nucleus. Such photons are absorbed only by very dense materials.

Neutrons have zero electric charge and, therefore, do not directly ionize matter; however, since they have a mass similar

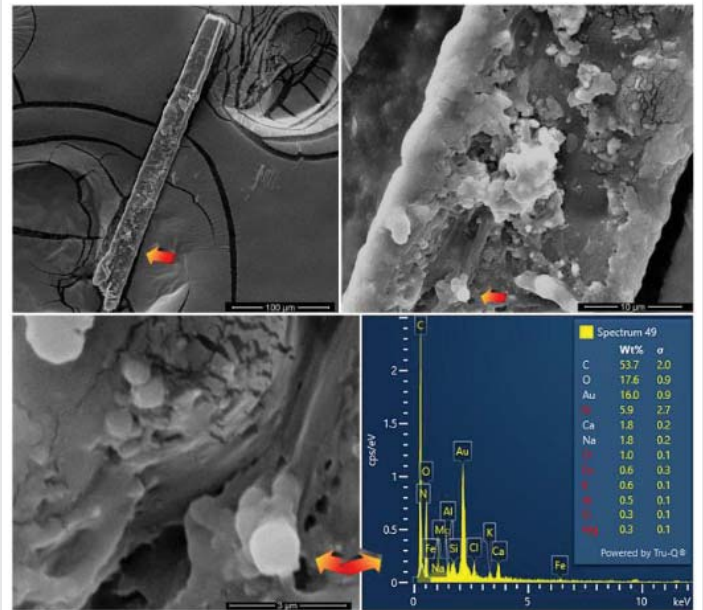


Figure 19: Three magnifications of stacked erythrocytes on a linen fiber coming from sticky tape 3EF. On the bottom right, elemental analysis via EDX showing the compatibility of the disk indicated with the arrow with bloody material. Gold-Au is evident, because the sample was previously metallized with Gold.

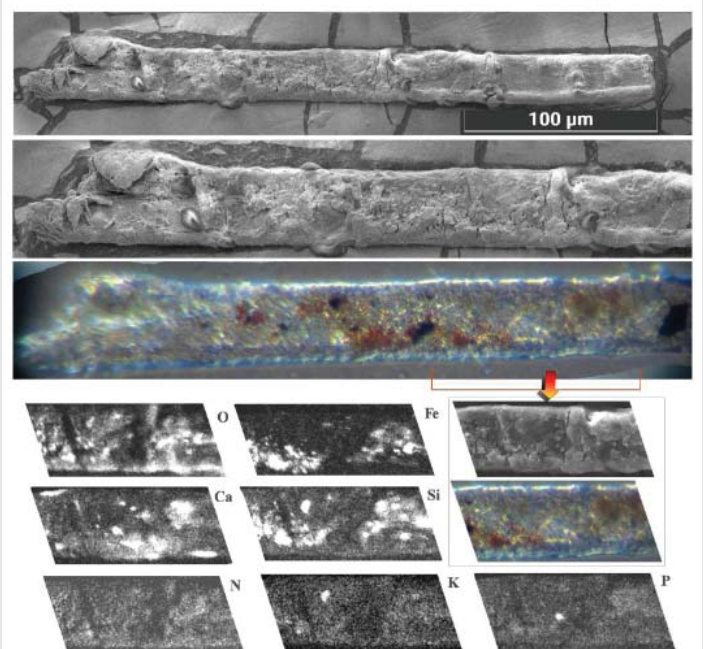


Figure 20: Map of some elements (Oxygen-O, Iron-Fe, Calcium-Ca, Silicon-Si, Nitrogen-N, Potassium-K and Phosphorus-P) present on the surface of fiber from sticky tape 3EF obtained by an SEM equipped with EDX analysis indicating the presence of clay, limestone, red ochre and cinnabar mixed with blood.

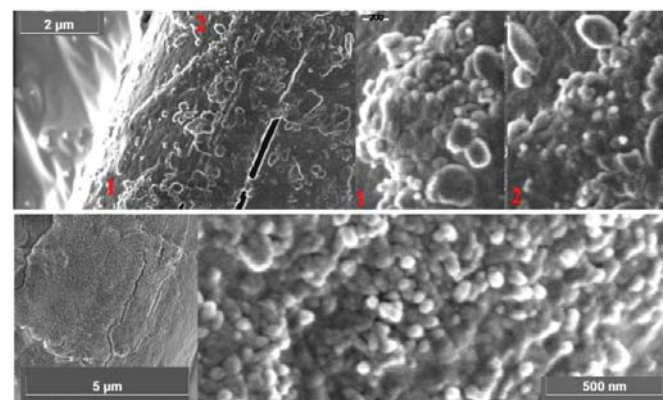


Figure 18: Nanoparticles recognized as creatinine in bloody fibers coming from Filter-h of dusts vacuumed from the back side of the gluteal area of the dorsal image of the HST.

to that of protons, they transfer their momentum entirely to them and, thus, ionize the atom. The products of the reaction, being very energetic, are very ionizing secondary radiations. Neutrons are blocked by collisions with other atoms.

In this preliminary study, an initial analysis is performed to determine whether there is a possible radiative activity of some type of HST blood particles. Given that the quantity of material available is extremely limited (in some cases also less

than a microgram), this analysis is not aimed at quantitative measurements of these hypothetical ionizing radiations nor at distinguishing the type of radiation, because the material used is sometimes not free, but drowned in the sticky tape's adhesive and/or protected from a microscope cover glass.

This study is, therefore, only aimed at answering the following question: *among the various ionizing radiations, is it possible to detect the presence of at least one without having to alter with invasive tests for the samples under examination?* As can be seen from the following Sections 6.1 and 6.2, these preliminary studies indicate an observable Beta-activity for Type A blood samples and a probable Gamma-activity for Type B samples.

6.1 Type A blood: Sample GF-1HB-2

Sample GF-1HB-2 described in Section 3 consists of bloody fibers placed on a microscope glass slide, immersed in balsam oil with a refractive index of 1.515, covered with a glass coverslip, and sealed with adhesive tape.

After having verified the negligible influence of the adhesive tape, the oil, and the linen fibers contained therein, the Beta-activity of the two glass slides and of the background noise was evaluated.

The Beta-activity measured after 7000 s was 903 counts, see Figure 21 [40], of which approximately 50% is attributable to Sample GF-1HB-2 and 30% to the support glass. Considering that the measured activity is proportional to the relative masses and considering that the mass of the supporting glass is several orders of magnitude larger than that of the sample under examination, it can be preliminarily concluded that the Beta-activity of the blood sample contained in the Sample GF-1HB-2 is several orders of magnitude larger than that of the support glass.

The Alpha-activity, also reported in the measurement of Figure 21, of 11 counts in 7000 s, was instead masked by the background noise and, therefore, considered not measurable in the current conditions. However, for this kind of activity, the effect of the filtering produced by the cover glass must be considered since, as previously reported, this activity is blocked even by a sheet of paper.

The possible Gamma-activity was, instead, masked by the background noise, also.

6.2 Type B blood: Sample GF-h18-a

Sample GF-h18-3a described in Section 3 consists of a sherd of blood (subsequently fractured in two parts) fixed on a sticky tape placed on a microscope slide.

The possible Alpha- and Beta-activity measured was masked by the background noise, while the Gamma-activity, was, instead, a bit over the background noise; therefore, to be better measured in the future, instruments should be used that have a lower background noise.



Figure 21: Alpha and Beta counting performed on Sample of blood GF-1HB-2 after 7000 s. On the left the sample put on the drawer of the measurement machine; on the center, a photomicrograph of the sample, and on the right, the resulting counting.

7. Fluorescence of blood

It is well known that bloodstains visible on HST have a reddish color which is not typical of ancient blood crusts. Many scholars have tried to provide explanations for this fact, but these hypotheses are not definitive.

Recently, A. Di Lascio, et al. [46] proposed the hypothesis of the effect of ultraviolet UV rays on the bilirubin in blood produced by the rupture of erythrocytes during heavy flagellation, with the consequent release of hemoglobin which would then be transformed through the action of liver enzymes into bilirubin.

Bilirubin is fluorescent and could explain, at least in part, the fluorescence found in Type A blood. However, a new alternative hypothesis could refer to what is described in Section 6 where the non-negligible Beta-activity found in this type of blood is discussed and which could have also altered the C14/1988 results.

Even alkalosis produced by an excessive content of urea in the blood due to renal failure [1] (with consequent hypokalemia or potassium deficiency, also produced by muscle spasms), hemolysis (that is the destruction of red blood cells with consequent poor oxygenation of tissues) and the echinocytes formation induced by pulses in an intense electric field (supposed for the body image formation [1]) should not be also forgotten both in reference to the possible hypothesis of echinocytes formation discussed in Section 5.1 and the production of free hemoglobin then transformed into fluorescent bilirubin.

The fluorescence of Type A HST blood is highlighted by Figure 22 which compares the orange-red color of an HST blood sherd with the dark color of a common human blood crust seen under ultraviolet radiation.

It probably escaped many scholars, but blood fluorescence was first detected by Gilbert & Gilbert during the STuRP campaign in 1978. In fact, a study [47] reports in Figure 14 where there is plotted the "Relative spectral reflectance of the mean of four blood-stained areas on the Shroud (wrist-F3E, Side-F6B, forehead 3 mark-F8C, and back-B3C)." a fluorescence relative peak at the wavelength of 610 nm with a corresponding relative reflectance value of 0.80 near values of 0.76. Figures 23 and 24 show other examples of fluorescence of Type A blood.

Type B blood, instead, does not show any kind of detectable fluorescence, see Figure 25. Finally, it is worth noting that in several cases of Type A blood, the particles recognized as shrunken erythrocytes are immersed in a fluid that appears semi-transparent in visible light but which shows a marked greenish fluorescence under UV like blood human serum, see Figure 26.

8. Comments on the blood under analysis at the light of Jesus' sufferings

The numerous news on hematic material have highlighted

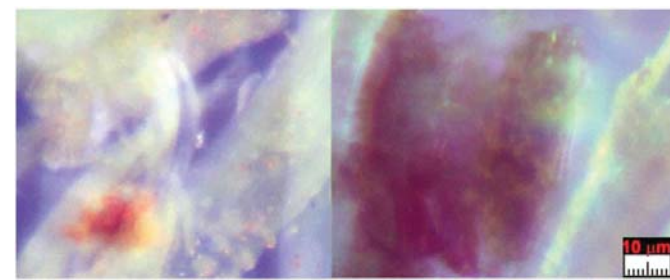


Figure 22: Fluorescence of a blood sherd coming from sample GF-1HB-2 of the HST, on the left, with the absence of fluorescence of a six-year-old human blood crust, on the right, both exposed to UV.

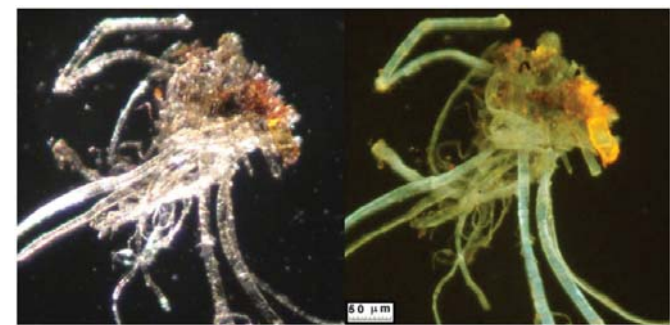


Figure 23: Bundle of TS fibers trapped within a blood crust coming from Filter-h taken in 1978, see Fig. 8 of Ref. [3]. On the left, we see it in reflected visible light, on the right, in UV. There we see the blue-greenish fluorescence of the linen fibers, and the red-orange fluorescence of the hematic material.

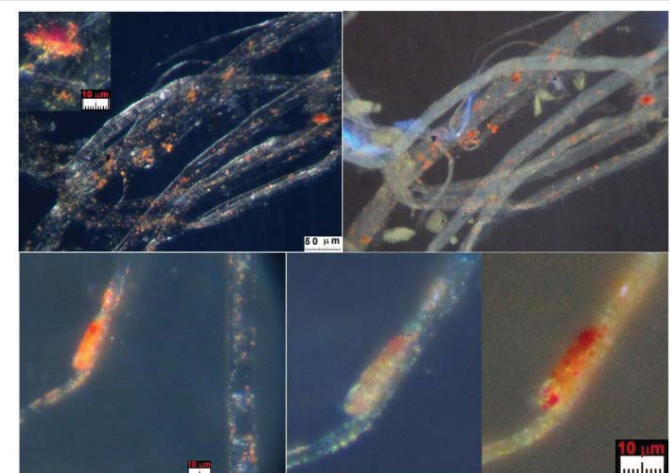


Figure 24: On the top, sample GF-1HB-2 of Type A blood as seen in reflected visible light on the left and in 365-nm-UV filtered by a high-pass filter at 400 nm on the right. On the bottom, a drop of hematic fluid that reached the linen fiber in the liquid phase, and sample GF-3EF-1 again seen in UV on the right.

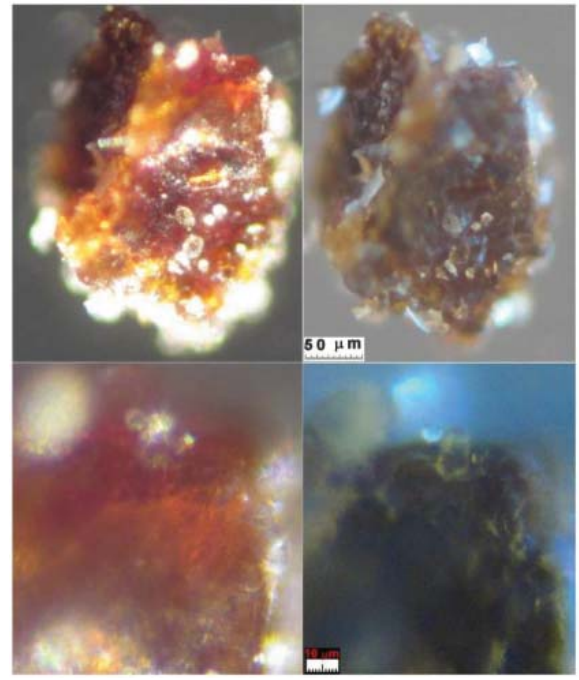


Figure 25: On the left, sample GF-h-18-3b of Type B blood as seen in reflected visible light at different magnifications, and, on the right, as seen in reflected 365-nm-UV where no fluorescence is detectable.

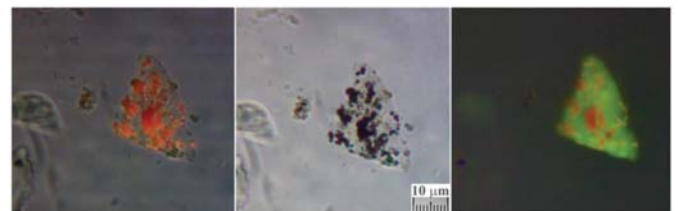


Figure 26: Hematic crust taken from sample GF-3EF-3 containing sub-micrometric particles of blood Type A, which is recognized as shrunken erythrocytes (or parts of them) in Section 5.1, dispersed or grouped in agglomerates. On the left, the hematic crust is seen in reflected visible light; on the center in transmitted visible light; on the right, the UV evidences the orange-red fluorescence of the blood particles with the greenish fluorescence of the supposed serum.

various features that will need to be explored more in-depth in the near future.

First of all, several very different types of blood have been highlighted which do not imply being from a different person, but, instead, suggest different moments or conditions of formation.

Very little can be said about Type C blood due to the limited material available. Type A blood is physically very different from Type B blood which may have coagulated on the skin before Jesus' death on the cross.

Unlike Type B, Type A blood shows fluorescence, Beta-activity, and a red-orange color atypical for ancient blood. It could have been transposed onto the HST when Jesus was in the sepulcher wrapped in the cloth. It is curious to observe that the description made by some mystics such as A. K. Emmerick and M. Valtorta of the luminous wounds of the Glorious Body of Jesus could be, in some way, confirmed by the atypical characteristics of this Type A blood.

On the basis of the features detected especially at a microscopic level for Type A blood (which, for the author, is from Jesus Christ), compared with the information on the Passion and Death of Jesus Christ from the Bible, it is interesting to formulate some working hypotheses of His various physical conditions during His last hour on the cross before His death.

Jesus was severely scourged especially at the kidneys, and nailed to the cross, He died, and His corpse was placed in the Sepulcher in Jerusalem and wrapped in the HST.

The high level of urea hypothesized in Type A blood implies renal (and probably of the liver too) malfunction or blockage which is a condition compatible with the intense flagellation found on the HST in the area of the kidneys [1], causing microcytic anemia. This microcytic anemia, also increased by prolonged fasting, suggests the extreme difficulties Jesus had in exchanging oxygen which most likely resulted in extremely labored breathing.

We must not forget the probable coagulopathy caused both by the excessive loss of blood and coagulation factors that occurred during the ferocious flagellation of Jesus Who probably lost at least a third of the volume of His blood thereby causing hypovolemic shock (a strong reduction in the volume of blood circulating in the body due to various hemorrhages and losses of body fluids especially produced as a result of His being flagellated).

Due to uremia, the red blood cells significantly reduced their ability to exchange oxygen, thus causing a notable tachycardia, which was also accentuated by tonic and clonic contractions, or muscle spasms, resulting from the hypertension of the limbs nailed to the cross. It is, therefore, easy to assume that Jesus' heart was beating very quickly due to congestive heart failure and also causing a pericardial effusion.

Therefore, the hypothesized high level of urea, important to explain the shrinkage of the erythrocytes of Type A blood and the high percentage of creatinine found in Figure 19, may be explained, especially during the Jesus' last hour before dying on the cross, by a reduced blood flow to the kidneys also caused by hypovolemia and by severe dehydration (confirmed by the Gospel of John [19:28] when records that "*Jesus said, I thirst.*").

In other words, the strong uremia that produced an accentuated shrinkage of the volume of the erythrocytes in the blood caused serious problems in oxygen exchange during breathing. To compensate for these physical problems in exchanging oxygen, Jesus had to heavily increase His breathing and, consequently, increase the frequency of His heartbeats, which prompted a heart attack as the main cause of His death.

During the deposition in the tomb, the corpse of Jesus was smeared with a mixture of oily substances containing aloë and myrrh (manteca), which additionally acted in shrinking the erythrocytes of the post-mortem blood Type A, that came out of the wound holes while the corpse was moved during preparation on the anointing stone.

The blood particles of this very particular Type A blood, even more than ten times smaller in diameter than those of a common human body, would correspond precisely to this blood impregnated on the HST in the sepulcher. The supposed kidney (and probably also liver) failure induced, among other, deterioration of platelet function that can better explain the relatively high quantity of post-mortal blood flowed by the wounds.

The Gospel of John (19:34) records that "*there came out blood and water.*" According to the author, this "*water*" was not only serum (which was already detected in correspondence of the bloodstains [26,27]) but probably pleural fluid deriving from intense pulmonary edema (it is an excess of liquids that accumulated in the pulmonary alveoli where oxygen exchanges between the air and the blood caused breathing problems); it is also in agreement with the results obtained from the analysis of the Sudarium of Oviedo (that hypothesizes the presence of fluids deriving from a pulmonary edema) which probably was caused by hemothorax (i.e. the laceration of the lung resulting from a blunt trauma perhaps caused by Jesus' having fallen while carrying the cross) of such intensity so as to put the right lung out of action and causing both pulmonary edema and a pleural effusion between the lung and the chest wall which compressed the lung from external pressure [48,49]. Finally, we must not forget the probable cardiogenic pulmonary edema that is caused by increased pressure in the heart, as mentioned above, due to tachycardia.

As suggested by many experts [15,48,49], all these causes accentuated the relatively early death of Jesus on the cross due to a hemopericardial infarction.

9. Conclusion

After a critical analysis of the main results obtained in the recent past on the hematic material of the HST, this paper presents various news regarding this hematic material on both a macroscopic and a microscopic level.

From a historical point of view, it is interesting to remember that the 1969 Pellegrino Commission identified and described in 1973-75 blood particles despite its not officially recognizing them as such, due to these particles being different and too shrunken when compared to those expected from a human body.

In 1980, Heller & Adler of STuRP and subsequently others analyzed similar material from a chemical point of view and identified it as blood, but without recognizing the presence of shrunken erythrocytes, which, instead, are described in this paper together with other peculiarities that are the following.

At a macroscopic level, the different directions of blood flow from the side wound are discussed, the probable presence of pulmonary fluid due to pulmonary edema from the side wound, the different kinds of hematic fluids from the left arm, some bloodstains out of the body image confirming the hypothesis of body image formation due to a human body floating on an intense electric field, the scourge marks corresponding to the

image of the head, and, finally, the volume of blood necessary to stain all the wounds present on the HST are experimentally quantified and commented on.

At a microscopic level, three different types of blood are distinguished -Type A, B, and C - with hypotheses formulated to account for their origin after describing their different characteristics. In particular, the hypothesis to consider the post-mortem Type A blood shed on the HST in the sepulcher when Jesus' body was wrapped in the HST is discussed. Type B blood, on the other hand, could consist of blood crusts that coagulated on the skin when Jesus was still alive.

However, as the quantity of material analyzed is too small, little can be said about Type C blood which probably consists of erythrocytes having sizes ranging from 2 to 5 micrometers.

The presence of fibrin, of earthy material, of creatinine typical of a tortured person, the stacking of erythrocytes probably produced by an electric field, and the Beta-activity and the fluorescence typical of Type A blood (but not of Type B blood) are also discussed.

Finally, the physical conditions relating to Jesus are discussed from a medical point of view which could explain all the news regarding the hematic material taken from the HST, especially the shrunken erythrocytes. All of these results are consistent with the description of Jesus Christ in the Holy Bible and, in particular, within the four Canonical Gospels.

Acknowledgement

The author heartily thanks the late Prof. Don Lieto Massignani who highly encouraged the writing of this paper; he also thanks the late Raymond Rogers and the late Giovanni Raggi di Numana for providing the author with material from the HST as well as all the persons and institutions that, subsequently, contributed to the supply of this material.

Thanks to Theodora A. Pappas of Shroud-Science Group for the useful advice and corrections regarding the English language made in this paper.

The author thanks prof. Rosa Boano and Prof. Ezio Fulcheri for the information regarding ancient erythrocytes, dr. August Accetta and Dr. Mary Hines (both of Shroud-Science Group), and Dr. Cristina Antonini for the useful medical advice. Finally, he thanks Dr. Ennio Paiaro for reviewing the medical aspects of this paper.

Funding

This research was partially supported by a religious group that requested anonymity and entrusted the author with the analysis of the so-called "*Padre Pio handkerchief*", a fabric on which two images considered miraculous are imprinted on the front and back, of HST-like Jesus Christ and Saint Pio of Petralcina respectively.

Biography

Giulio Fanti has been an associate professor of Mechanical and Thermal Measurements at the Department of Industrial Engineering of the University of Padua since 1996.

He was a founding member of the Interdepartmental Center for Space Studies and Activities "CISAS G.

Colombo" and a member of international groups for important space missions.

He has been dealing with the HST for more than twenty-five years and for more than twenty years he has been coordinator of the Shroud Science Group (which has around a hundred mostly American scholars). He was a member of the Scientific Committee of several conferences and coordinator of a University Research Project on the HST financed by the University of Padua.

His current research activity is mainly aimed at explaining the formation of the body image (still not reproducible today) and at dating the most important Relic of Christianity.

He is the author of more than two hundred works including books, educational texts, and publications in important Italian and international journals, most of which are on HST topics.

References

1. Fanti G. Holy Fire and Body Image of the Holy Shroud: Divine Photography Hypothesis. *World Scientific News WSN*. 2023;176:104-120. Available from: <https://realseekerministries.wordpress.com/wp-content/uploads/2023/01/new-giulio-fanti-holy-fire-divine-photo-hypothesis.pdf>
2. Fanti G. Could an anomaly in Turin Shroud blood reopen the 1988-radiocarbon dating result? *World Scientific News*. 2021;162:102-119. Available from: <https://realseekerministries.wordpress.com/wp-content/uploads/2022/04/giulio-fanti-blod-and-1988-xarbon-dating-refuted.pdf>
3. Fanti G. A Reexamination of the Pigment-Reinforcement Hypothesis of the Turin Shroud's Bloodstains. *World Scientific News*. 2022;163:99-114. Available from: <https://worldscientificnews.com/a-reexamination-of-the-pigment-reinforcement-hypothesis-of-the-turin-shrouds-bloodstains/>
4. Jumper EJ, Adler AD, Jackson JP, Pellicori SF, Heller JH, Druzik JR. A comprehensive examination of the various stains and images on the Shroud of Turin. *Archaeological Chemistry III, ACS Advances in Chemistry* 205. 1984;22:447-476. Available from: <https://www.semanticscholar.org/paper/A-comprehensive-examination-of-the-various-stains-Jumper-Adler/1eae56c3ef4c1e5486b45660a0a13d23f3df38ba>
5. Schwalbe LA, Rogers RN. Physics and chemistry of the Shroud of Turin, a summary of the 1978 investigation. *Analytical Chemical Acta*. 1982;135:3-49. Available from: <https://ui.adsabs.harvard.edu/abs/1982AcAC..135....3S/abstract>
6. Jumper EJ, Mottern RW. Scientific investigation of the Shroud of Turin. *Applied Optics*. 1980;19(12):1909-1912. Available from: <https://pubmed.ncbi.nlm.nih.gov/20221154/>
7. Mottern RW, London RJ, Morris RA. Radiographic Examination of the Shroud of Turin - a Preliminary Report. *Materials Evaluation*. 1980;38(12):39-44. Available from: <https://www.shroud.com/pdfs/Radiographic%20Examination%20Preliminary%20Report%20Mottern%20London%20Morris%201979%20OCRsm.pdf>
8. Morris RA, Schwalbe LA, London JR. X-ray fluorescence investigation of the Shroud of Turin. *X-Ray Spectrometry*. 1980;9(2):40-7. Available from: <https://www.semanticscholar.org/paper/X-ray-fluorescence-investigation-of-the-shroud-of-Morris-Schwalbe/285247d90580b1f4fb3bf18864a8425ae4e9f211>
9. Fanti G. Open issues regarding the Turin Shroud. *Scientific Research and Essays*. 2012;7(29):2507. Available from: https://academicjournals.org/article/article1380797290_Fanti.pdf



10. Fanti G. Hypotheses regarding the formation of the body image on the Turin Shroud. A critical compendium. *J Imaging Sci Technol.* 2011;55(6):060507. Available from: <http://dx.doi.org/10.2352/J.ImagingSci.Technol.2011.55.6.060507>
11. Fanti G, Maggiolo R. The Double Superficiality of the Frontal Image of the Turin Shroud. *J Opt A: Pure Appl Opt.* 2004;6:491-503. Available from: https://astro1.panet.utoledo.edu/~ljc/shroud_rev.pdf
12. De Caro L, Barta C, Fanti G, Matricciani E, Sibillano T, Giannini C. Long-Term Temperature Effects on the Natural Linen Aging of the Turin Shroud. *Information.* 2022;13(10):458. Available from: <https://doi.org/10.3390/info13100458>
13. Fanti G. Can Corona Discharge explain the body image formation of the Turin Shroud? *J Imaging Sci Technol.* 2010;54(2):020508-1/10. Available from: <http://dx.doi.org/10.2352/J.ImagingSci.Technol.2010.54.2.020508>
14. McAvoy T. Shroud of Turin ultraviolet light images: color and information content. *Appl Opt.* 2021;60(22). Available from: <https://opg.optica.org/ao/abstract.cfm?uri=ao-60-22-6604>
15. Bevilacqua M, Fanti G, D'Arienzo M. New Light on the Sufferings and the Burial of the Turin Shroud Man. *Open J Trauma.* 2017;1(2):047-053. Available from: <http://dx.doi.org/10.17352/ojt.000010>
16. Damon PE, Donahue DJ, Gore BH, Hatheway AL, Jull AJT, Linick TW, et al. Radiocarbon dating of the Shroud of Turin. *Nature.* 1989;337:611-615. Available from: <https://www.nature.com/articles/337611a0>
17. Riani M, Atkinson AC, Fanti G, Crosilla F. Regression analysis with partially labelled regressors: carbon dating of the Shroud of Turin. *Stat Comput.* 2013;23:551-561. Available from: <https://link.springer.com/article/10.1007/s11222-012-9329-5>
18. Rogers RN. Studies on the Radiocarbon Sample from the Shroud of Turin. *Thermochim Acta.* 2005;425:189-194. Available from: <http://www.shroud.it/ROGERS-3.PDF>
19. Phillips TJ. Shroud irradiated with neutrons? *Nature.* 1989;337:16. Available from: https://staff.polito.it/alberto.carpinteri/related%20piezonuclear%20papers/337594a0_mod.pdf
20. Hedges REM. Reply to Shroud irradiated with neutrons? *Nature.* 1989;337:16. Available from: <https://www.nature.com/articles/337594a0>
21. Schwalbe L, Walsh B. On Cleaning Methods and the Raw Radiocarbon Data from the Shroud of Turin. *Int J Archaeol.* 2021;9(1):10-16. Available from: <https://www.sciencepublishinggroup.com/article/10.11648/j.ija.20210901.12>
22. McAvoy T. On Radiocarbon Dating of the Shroud of Turin. *Int J Archaeol.* 2021;9(2):34-44. Available from: <https://www.sciencepublishinggroup.com/article/10.11648/j.ija.20210902.11>
23. Hedges REM. Sample Handling in Radiocarbon Dating by Accelerator with Special Reference to the Turin Shroud. *Anal Proc.* 1990;27:45.
24. Enoto T, Wada Y, Furuta Y, Nakazawa K, Yuasa T, Okuda K, et al. Photonuclear reactions triggered by lightning discharge. *Nat Lett.* 2017;483:24630. Available from: <https://pubmed.ncbi.nlm.nih.gov/29168803/>
25. Fanti G, Zagotto G. Blood reinforced by pigments in the reddish stains of the Turin Shroud. *J Cult Heritage.* 2017;25:113-120. Available from: <https://www.sciencedirect.com/science/article/abs/pii/S1296207417300092>
26. Heller JH, Adler AD. Blood on the Shroud of Turin. *Appl Opt.* 1980;19(16):2742-2744. Available from: <https://www.shroud.com/pdfs/Blood%20on%20The%20Shroud%20Heller%20Adler%201980%20OCR.pdf>
27. Heller JH, Adler AD. A Chemical Investigation of the Shroud of Turin. *Can Soc Forensic Sci J.* 1981;14(3):81-103. Available from: <https://doi.org/10.1080/00085030.1981.10756882>
28. Svensson N, Heimburger T. Forensic aspects and blood chemistry of the Turin Shroud Man. *AJ Sci Res Essays.* 2012;7(29):2513-2525. Available from: <https://academicjournals.org/journal/sre/article-full-text-pdf/080a92329177>
29. Baima Bollone PL. Indagini identificative su fili della Sindone. *Giornale della Accademia di Medicina di Torino.* 1982;(1-12):228-239.
30. Lucotte G. *Vérités sur le Saint Suaire.* Anet: Atelier Fol'fer; 2010.
31. McCrone WC, Skirius C. Light Microscopical Study of the Turin 'Shroud,' I. The Microscope. 1980;28:105. Available from: <https://scirp.org/reference/referen cespapers?referenceid=1869596>
32. McCrone WC. Light microscopical study of the Turin „Shroud” II. *The Microscope.* 1980;28(4):115-120.
33. McCrone WC. Light microscopical study of the Turin „Shroud” III. *The Microscope.* 1981;29(1):19-39.
34. McCrone WC. The Shroud of Turin: blood or artist's pigment? *Acc Chem Res.* 1990;23:77-83. Available from: <https://pubs.acs.org/doi/10.1021/ar00171a004>
35. McCrone WC. *Judgement day for the Turin Shroud.* Chicago, USA: The Microscope Pub.; 1997.
36. McCrone WC. Shroud 1999. *The Microscope.* 1999;47(1):55-61.
37. McCrone WC. The Shroud Image. *The Microscope.* 2000;48(2):79-85.
38. Baima Bollone P, Marino C, Pescarmona G. Il significato del colore delle macchie di sangue della Sindone ed il problema della bilirubina. *Sindon Nuova Serie.* 2001;(15):19-29
39. Goldoni C. The Shroud of Turin and the bilirubin blood stains. *Ohio Shroud Conference.* 2008. Available from: <http://www.shroud.com/pdfs/ohiogoldoni.pdf>
40. ALPHA-BETA COUNTING SYSTEMS ALBA 2000 series. Available from: http://www.elsenuclear.com/media/k2/attachments/DAT_ALBA_EN_1.01.pdf
41. Fanti G, Malfi P. *The Shroud of Turin, First Century After Christ!* Singapore: Jenny Stanford Pub. 2020. Available from: <https://doi.org/10.1201/9780429468124>
42. Brillante C, Fanti G, Marinelli E. Bloodstains characteristics to be considered in laboratory reconstruction of the Turin Shroud. *IV Int. Symposium, Paris.* 2002. Available from: <http://www.sindone.info/BRILLAN2.PDF>
43. Kohlbeck JA, Nitowski EL. New Evidence May Explain Image on Shroud of Turin. *Chemical tests link Shroud to Jerusalem.* *Biblic Archaeol Rev.* 1986;12(4):18-29. Available from: <https://www.scirp.org/reference/reference spapers?referenceid=1619702>
44. Rabino-Massa E, Chiarelli B, Sacerdote M, Focale C. Presence of red blood cells in the tissues of Egyptian mummies. *J Biol Res - Bulletin of the Italian Society of Experimental Biology.* 1967;XLIII:20.
45. Carlino E, De Caro L, Giannini C, Fanti G. Atomic resolution studies detect new biologic evidences on the Turin Shroud. *PLoS One.* 2017;12(6). Available from: <https://doi.org/10.1371/journal.pone.0180487>
46. Di Lascio A, Di Lazzaro P, Iacomussi P, Missori M, Murra D. Investigating the color of the blood stains on archaeological cloths: the case of the Shroud of Turin. *Appl Opt.* 2018;57(23):6626-6631. Available from: <https://doi.org/10.1364/AO.57.006626>
47. Gilbert R Jr, Gilbert MM. Ultraviolet-visible reflectance and fluorescence spectra of the Shroud of Turin. *Appl Opt.* 1980;19(12):1930-1936. Available from: <https://doi.org/10.1364/AO.19.001930>
48. Bevilacqua M, Fanti G, D'Arienzo M, De Caro R. Do we really need new medical information about the Turin Shroud? *Injury.* 2014;45(2):460-464. Available from: <https://doi.org/10.1016/j.injury.2013.09.013>
49. Bevilacqua M, Fanti G, D'Arienzo M. The Causes of Jesus' Death in the Light of the Holy Bible and the Turin Shroud. *Open J Trauma.* 2017;1:37-46. Available from: <http://dx.doi.org/10.17352/OJT.000009>